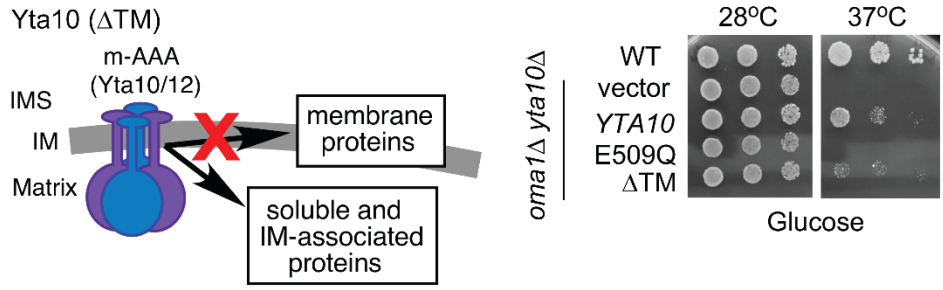

Figure S1. Simultaneous loss of Oma1 and Yta10 impairs proteolysis of intrinsic IM proteins. Left, schematic depiction of functional impairment in the m-AAA protease harboring the Yta10(ΔTM) subunit lacking transmembrane segments. Right, fermentative growth of WT or *oma1*Δ *yta10*Δ cells expressing the indicated Yta10 variants, handled and analyzed as in Figure 1A.

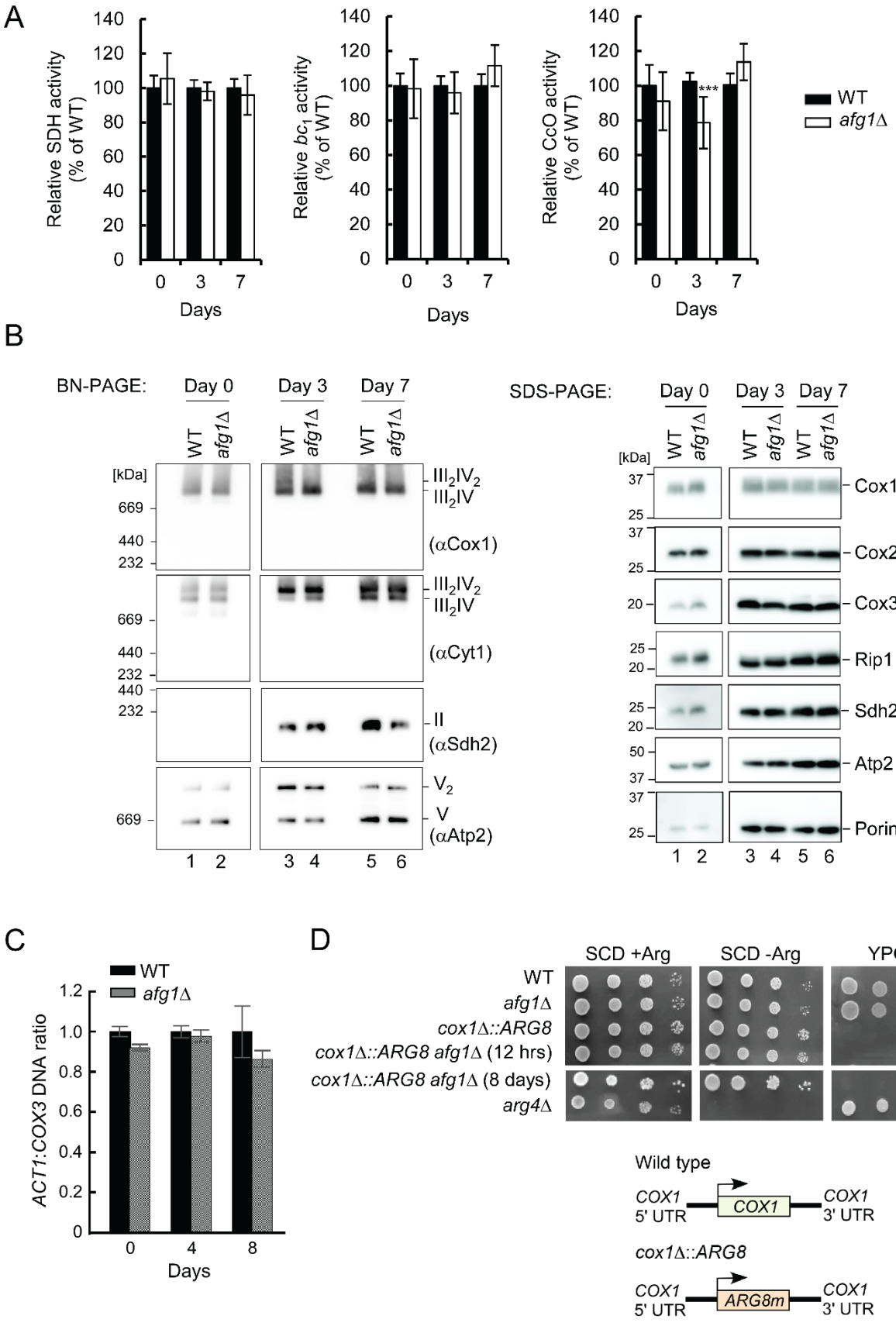

Figure S2. ETC enzymatic activities, complexes, and subunits in the absence of Afg1 are similar to WT, and cells lacking Afg1 retain mitochondrial genome with aging, similarly to WT. (A) Succinate dehydrogenase (SDH), cytochrome bc_1 complex (bc_1), and cytochrome *c* oxidase (CcO) specific enzymatic activities in mitochondria from WT and *afg1*Δ cells isolated at indicated growth times, shown as a percentage of WT activity. Data are mean ± S.D. (n=3 biological replicates, each with n=3-4 technical replicates; ***p<0.001 by one-way ANOVA). (B) Left, Blue native (BN)-PAGE immunoblot analysis of respiratory complexes in mitochondria from cells isolated at indicated growth times, detected with indicated antibodies. Right, SDS-PAGE immunoblot analysis of representative subunits of respiratory complexes IV (CcO; Cox1-3), III (bc_1; Rip1), II (SDH; Sdh2), and V (Atp2) and loading control (Porin) in mitochondria from these cells. (C) Mitochondrial DNA copy number of WT and *afg1*Δ strains grown in SC-glucose medium for the indicated number of days and analyzed by qPCR. The copy number was calculated as the nuclear (*ACT1* gene) to mitochondrial (*COX3* gene) DNA ratio and was set equal to one for WT samples. Data are mean values ± SD of 3 independent experiments, each with n=3 technical replicates. (D) Translation of the *COX1* ORF from the mitochondrial genome in young (12 hours post-inoculation) and aged (8 days post-inoculation) WT and *afg1*Δ cells, assessed by deleting *AFG1* in the *cox1*Δ*::ARG8* genetic reporter strain depicted schematically. Cells were cultured in SC-glucose medium supplemented with low amounts (4 mg/L) of arginine for the indicated periods of time and spotted onto SC-glucose (SCD) plates with (+Arg) or without (-Arg) arginine as well as on yeast extract-peptone-glycerol/lactate (YPGL) plates. The *arg4*Δ mutant served as a control. Plates were incubated for 3 (SCD plates) or 4 (YPGL plates) days at 28°C before photography. UTR, untranslated region.

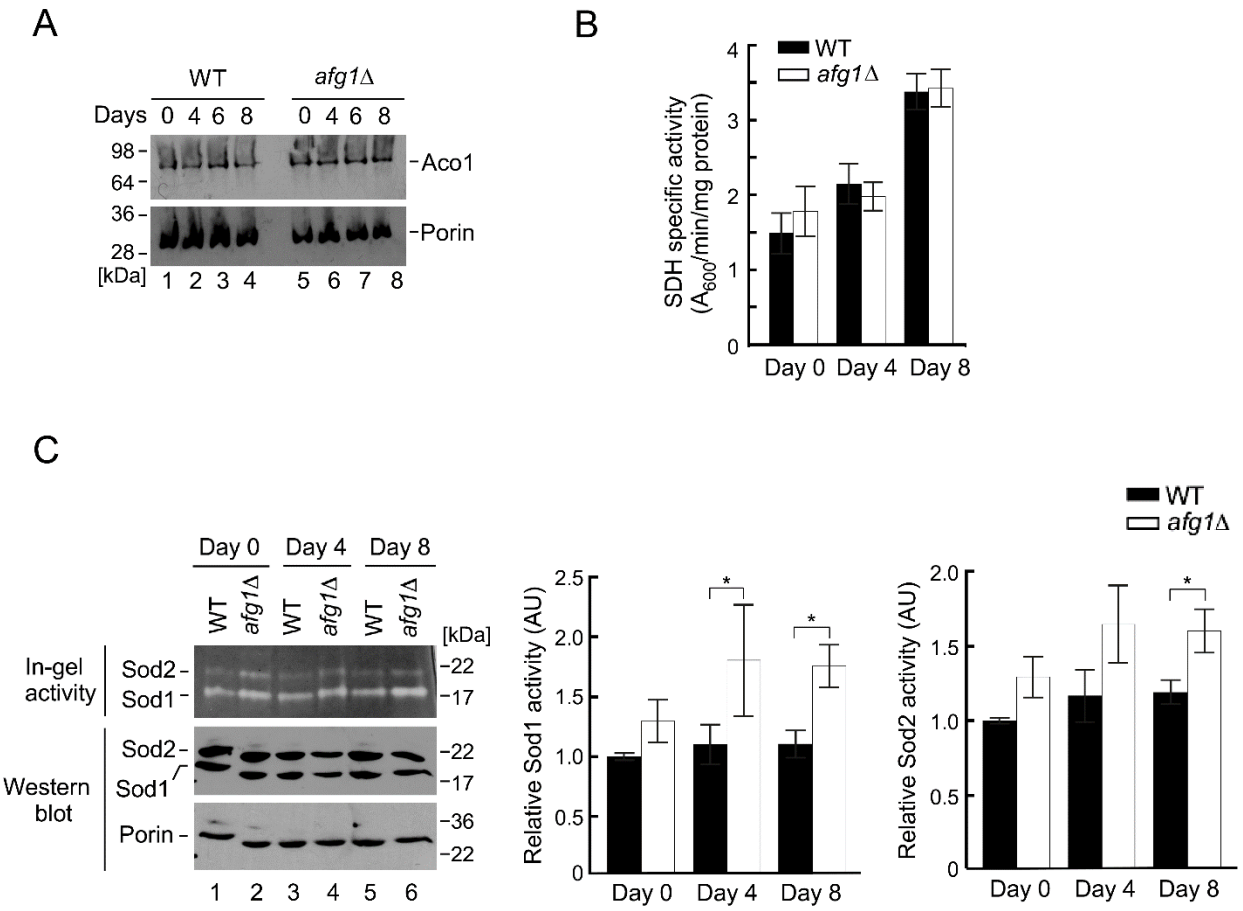

Figure S3. Loss of Afg1 does not impair aconitase steady-state levels or succinate dehydrogenase activity, while superoxide dismutase activity is elevated in aged cells lacking Afg1. (A) SDS-PAGE immunoblot analysis of the steady-state levels of aconitase (Aco1) and porin (loading control) in mitochondria described in Figure 3B. (B) Succinate dehydrogenase (SDH) enzymatic activity in mitochondria isolated from log-phase and 4- and 8-day-old WT and *afg1*Δ cells. Data are mean values ± SD of 3 independent experiments, each with n=3 technical replicates. (C) In-gel analysis of superoxide dismutase activity following native electrophoresis and assessment of steady-state levels of Sod1, Sod2, and porin following SDS-PAGE in the mitochondria described in Figure 3B. Quantitation of Sod1 and Sod2 in-gel staining signals is mean ± SD of 3 independent experiments, each with n=3 technical replicates; *p<0.05 by *t*-test.

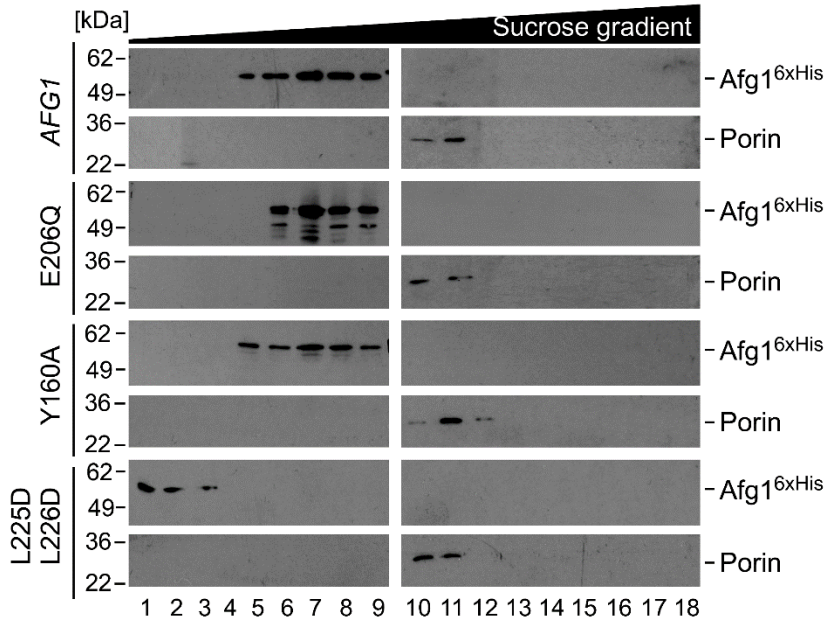

Figure S4. E206Q and Y160A variants of Afg1 are able to oligomerize. High-velocity fractionation of mitochondrial proteins from *afg1*Δ cells expressing Afg1-6xHis or its E206Q, Y160A, or L225D L226D variants solubilized with 1% digitonin. Following centrifugation on continuous sucrose density gradients (12-50%), gradient fractions were collected and analyzed by SDS-PAGE for distribution of Afg1 oligomers using anti-His antibody. The migration pattern of the 440-kDa porin complex (visualized with anti-porin antibody) was used for size comparison.

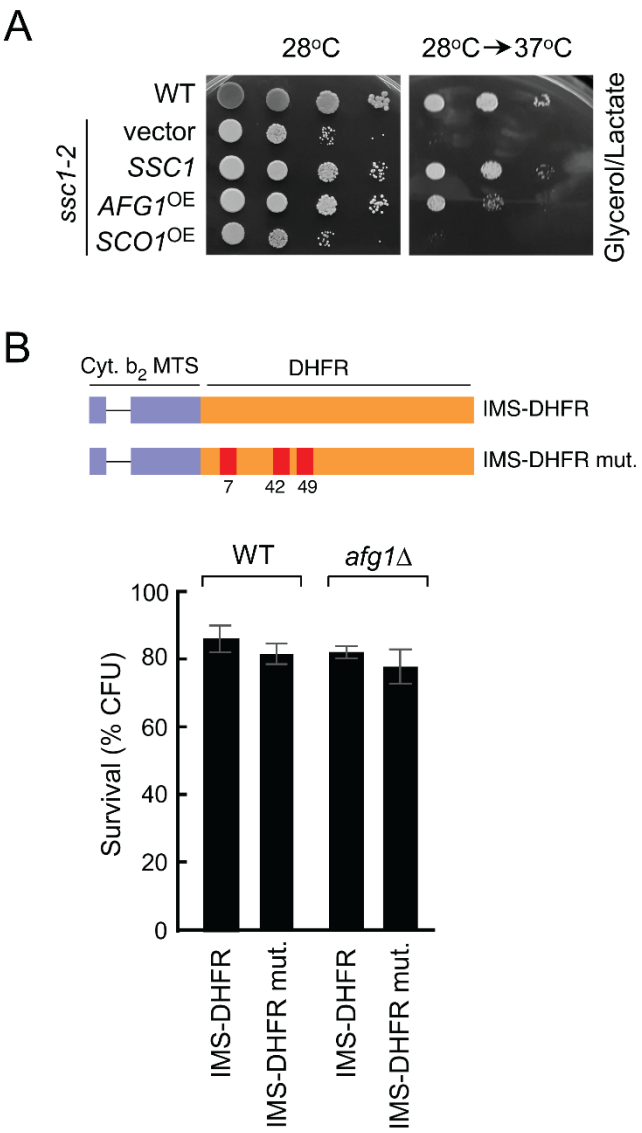

Figure S5. Afg1 over-expression partially compensates for the *ssc1-2* mutation, and a misfolding-prone protein targeted to the IMS in *afg1*Δ does not induce the growth defect observed for the matrix-targeted version. (A) Respiratory growth of WT and *ssc1-2* cells expressing vector control or *SSC1* or overexpressing *AFG1* or *SCO1* (negative control). Cells were handled as described in Figure 1A. (B) Top, schematic depiction of IMS-targeted DHFR chimeric protein consisting of the mitochondrial targeting/sorting moiety of yeast cytochrome b_2 (Cyt. b_2) fused to wild type (IMS-DHFR) or the misfolding-prone C7A, S42C, N49C variant of mouse DHFR (IMS-DHFR mut.). Bottom, colony viability of the indicated WT and *afg1*Δ transformants, assessed as described in Figure 5E. Data are mean values ± SD of 3 biological replicates, each with n=3 technical replicates.

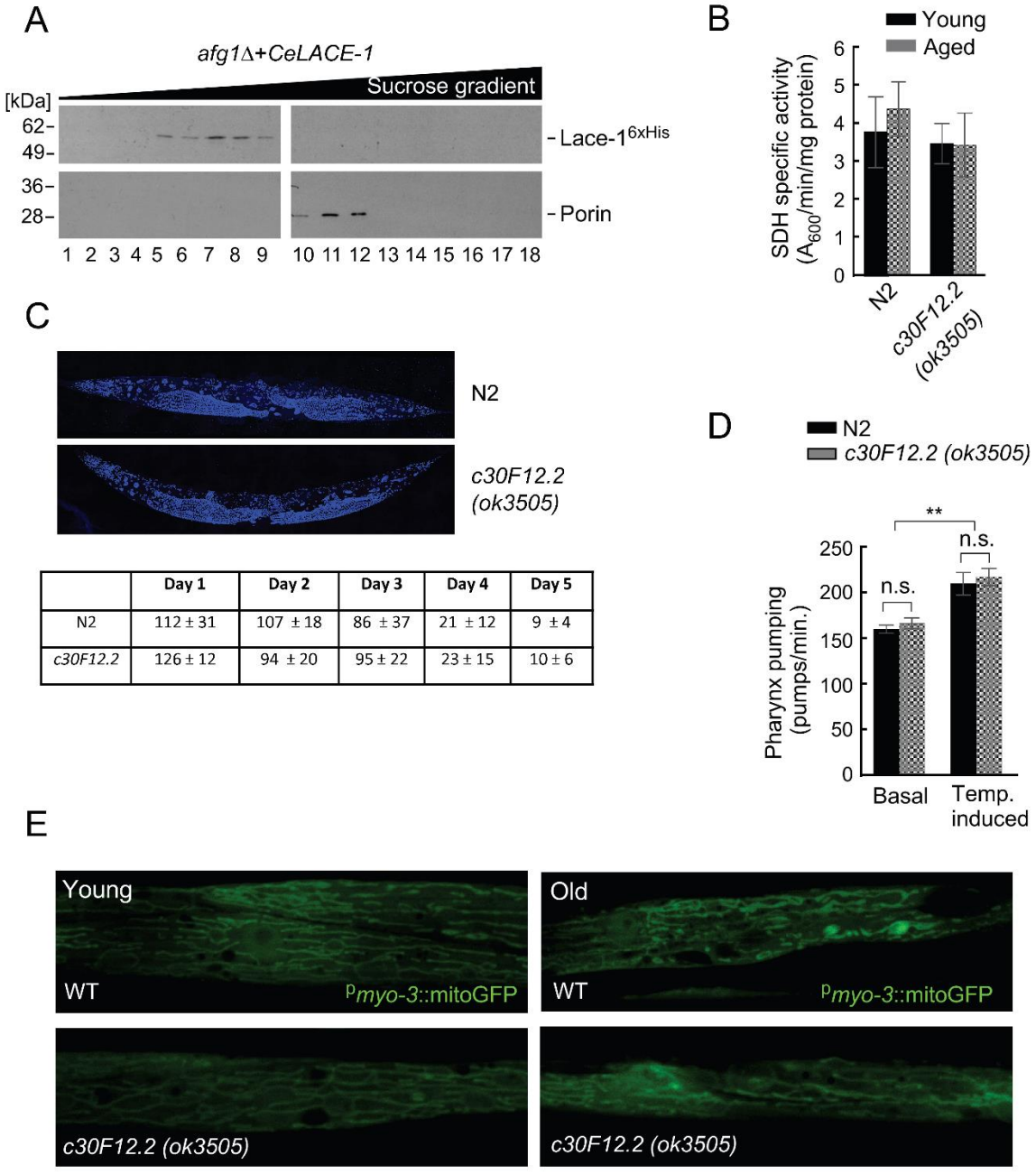

	Day 1	Day 2	Day 3	Day 4	Day 5
N2	112 ± 31	107 ± 18	86 ± 37	21 ± 12	9 ± 4
c30F12.2	126 ± 12	94 ± 20	95 ± 22	23 ± 15	10 ± 6

Figure S6. LACE-1 forms complexes similar to Afg1; worms lacking LACE-1 exhibit normal SDH activity, normal developmental phenotypes, normal basal and temperature-induced pharyngeal pumping rates, and normal muscle tissue mitochondrial networks.

(A) Density gradient fractionation of digitonin-solubilized mitochondria from yeast *afg1*Δ cells expressing C-terminally 6xHis-tagged *C. elegans* LACE-1 (*CeLACE-1*). The lysates were handled and analyzed as in Figure S4. (B) Enzymatic activity of succinate dehydrogenase in

mitochondria isolated from 1-day-old (young) and 5-day-old (aged) N2 and *c30F12.2(ok3505)* worms. Data are mean values ± SD (n=3 biological replicates with 3 animals per group). (C) Top, confocal micrographs (projected Z-sections) showing DAPI-stained N2 and *c30F12.2(ok3505)* animals. Bottom, average brood size of N2 animals and *c30F12.2(ok3505)* animals over 5 days. (D) Frequency of basal and temperature-induced pharynx movement (pumping) per minute in age-matched N2 and *c30F12.2(ok3505)* animals at day 1; n=3 with 10 animals per group. Data are mean values ± S.E.M.; n.s., not significant, **p<0.01 by *t*-test. (E) Representative fluorescence images of body wall muscle in age-matched WT and *c30F12.2(ok3505)* animals expressing ^{P}*myo-3::mitoGFP* mitochondria-targeted reporter at day 1 (young) and day 5 (old).

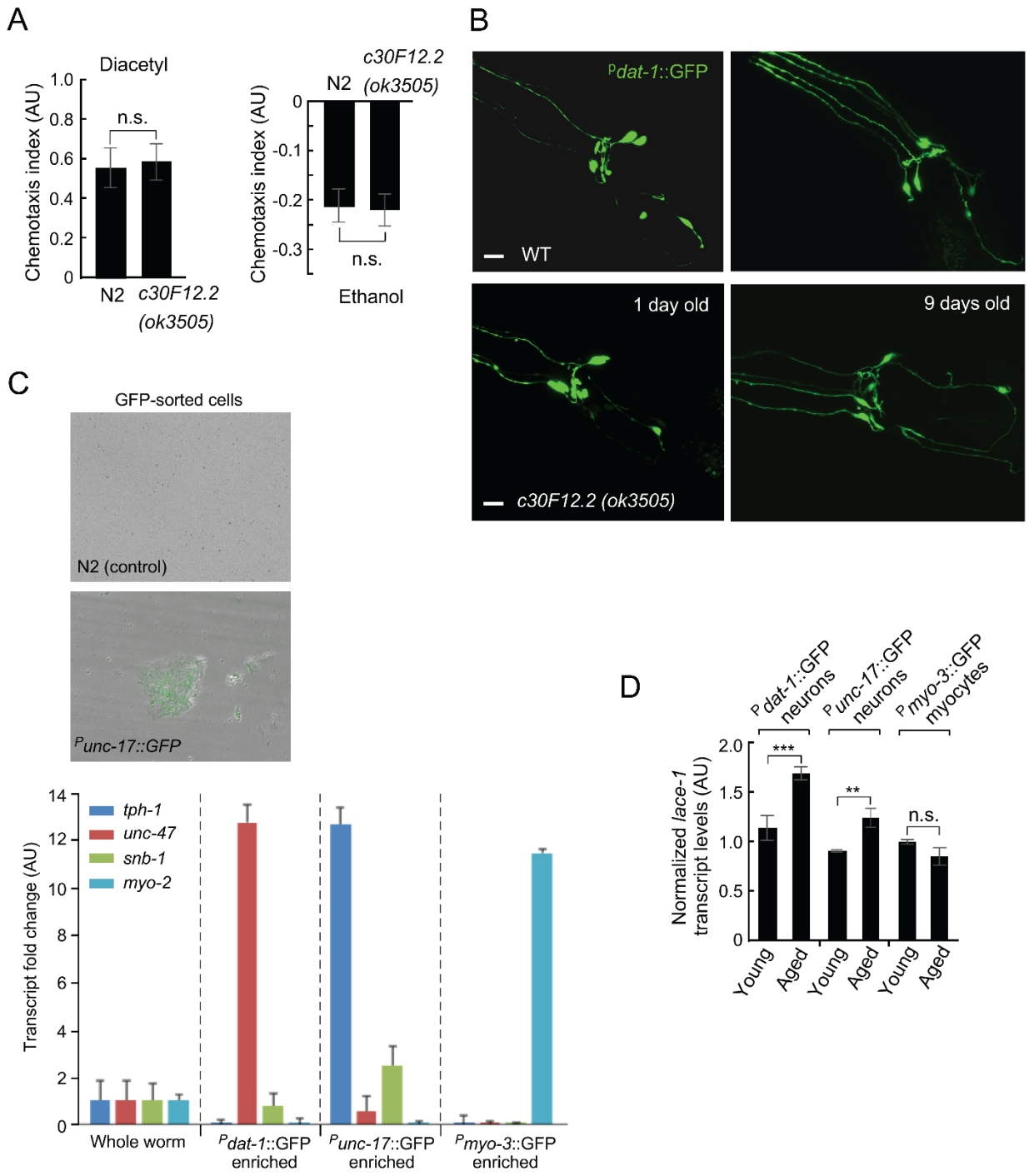

Figure S7. Worms lacking LACE-1 exhibit normal chemosensing and normal dopaminergic neurons; qPCR validates cell type following the isolation of GFP-sorted cells; worms exhibit increased expression of *lace-1* in neurons but not myocytes with aging. (A) Chemotaxis index of N2 and *c30F12.2(ok3505)* animals at Day 1. Worm responses

were tested for both attractive (diacetyl) and repulsive (ethanol) odorants; n=3 with 20 animals per group. Data are mean values ± S.E.M.; n.s., not significant by *t*-test. (B) Representative fluorescence images of dopaminergic neurons in 1-day-old (left) and 9-day-old (right) adult WT and *c30F12.2(ok3505)* animals expressing ^{P}*dat-1::*GFP reporter. (C) qPCR analysis of transcripts for the genes *tph-1*, *unc-47*, and *snb-1* (markers for neurons), and *myo-2* (marker for myocytes) and epifluorescent microscopy images showing the presence of GFP in the isolated cells. Image shows a single focal plane. (D) Transcript levels of *lace-1* in dopaminergic ^{P}*dat-1::GFP* neurons, cholinergic ^{P}*unc-17::GFP* neurons, and ^{P}*myo-3::GFP* myocytes isolated from relevant 1-day-old (young) and 5-day-old (aged) WT transgenic animals. Data are mean values ± SD (n=4 biological replicates with 4 animals per group; n.s., not significant, **p<0.01, ***p<0.001 by *t*-test).

Table S1. Yeast strains used in this study

Strain	Genotype	Reference/Source
W303-1B	*MATα ade2-1 can1-100 his3-11, 15 leu2-3, 112 trp1-1 ura3-1*	ATCC
W303-1B *afg1* Δ	*MATα ade2-1 can1-100 his3-11, 15 leu2-3, 112 trp1-1 ura3-1 afg1Δ::URA3MX*	This Study
W303-1B *oma1* Δ	*MATα ade2-1 can1-100 his3-11, 15 leu2-3, 112 trp1-1 ura3-1oma1Δ::HIS3MX6MX*	Bohovych et al., 2014
afg 1Δ *oma1* Δ	*MATα ade2-1 can1-100 his3-11, 15 leu2-3, 112 trp1-1 ura3-1 afg1Δ oma1Δ::URA3MX*	This Study
W303-1B *yta1* 0Δ	*MATα ade2-1 can1-100 his3-11, 15 leu2-3, 112 trp1-1 ura3-1 yta10Δ::HIS3MX6*	B. Meunier
yta10Δ oma1Δ	*MATα ade2-1 his3-1,15 leu2-3,112 trp1-1 ura3-1 yta10Δ::HIS3MX6 oma1Δ::TRP1*	This study
MB3 (*tim23-2*)	MATα ade2-101 his3-Δ200 leu2-Δ1 lys2-801 ura3::LYS2 tim23-2	N. Pfanner
cox1 Δ::ARG8	*MATα lys2 leu2-3, 112 arg8::hisG, ura3-52 [cox1Δ::ARG8m]*	Perez-Martinez et al., 2003
cox1 Δ::ARG8 *afg1* Δ	*MATα lys2 leu2-3, 112 arg8::hisG, ura3-52 [cox1Δ::ARG8m] afg1::URA3MX*	This study
DTY 833 (*arg4Δ)*	*MATa ade1Δ arg4Δ aro2Δ his7Δ lys5Δ ura2Δ*	D. Winge
MB4-1b *(sod2Δ)*	*MATa leu2-3,112 trp1-1 can1-100 ura3-1 ade2-1 his3-11,15 sod2Δ::KanMX*	A. Barrientos
afg 1Δ *sod2* Δ	*MATα ade2-1 can1-100 his3-11, 15 leu2-3, 112 trp1-1 ura3-1 afg1ΔSod2Δ::URA3MX*	This Study
PK81 (Ssc1-2)	*MATα his4-713 lys2 ura3-52 Δtrp1 leu2-3,112 ssc1-2::LEU2*	A. Barrientos
AFG1::6His	*MATα ade2-1 can1-100 his3-11, 15 leu2-3, 112 trp1-1 ura3-1 AFG1-His6::URA3MX*	This Study
AFG1::6His afg1Δ	*MATα ade2-1 can1-100 his3-11, 15 leu2-3, 112 trp1-1 ura3-1 AFG1-His6::URA3MX afg1Δ*	This Study
AFG1::6His yta10Δ oma1Δ	*MATa ade2-1 his3-1,15 leu2-3,112 trp1-1 ura3-1 AFG1-His6::URA3MX yta10Δ::HIS3MX6 oma1Δ::TRP1*	This study
AFG1::6His PK81	*MATα his4-713 lys2 ura3-52 Δtrp1 leu2-3,112 ssc1-2::LEU2 AFG1-His6::URA3MX*	This Study
SSC1::6His PK81	*MATα his4-713 lys2 ura3-52 Δtrp1 leu2-3,112 ssc1-2::LEU2 SSC1-His6::URA3MX*	This Study
SCO1::HA PK81	*MATα his4-713 lys2 ura3-52 Δtrp1 leu2-3,112 ssc1-2::LEU2 SCO1-HA::HIS3*	This Study